# Comparison of Electrostatic Interactions and of Protein–Protein Orientations in Electron-Transfer Reactions of Plastocyanin with the Triplet State of Zinc Cytochrome *c* and with Zinc Cytochrome *c* Cation Radical†

Jian S. Zhou and Nenad M. Kostić *

*Department of Chemistry, Iowa State University, Ames, Iowa 50011*

*Received September 16, 1992; Revised Manuscript Received February 18, 1993*

ABSTRACT: Photoinduced reduction of cupriplastocyanin by the triplet state of zinc cytochrome *c* (the "forward" reaction) and the subsequent thermal oxidation of cuproplastocyanin by zinc cytochrome *c* cation radical (the "back" reaction) at ionic strengths from 40 mM to 3.00 M are studied by laser kinetic spectroscopy (so-called flash photolysis). Variation of the bimolecular rate constants over the entire range of ionic strength cannot be explained in terms of monopole–monopole interactions between the protein molecules, but it can be explained in terms of monopole–monopole, monopole–dipole, and dipole–dipole interactions. Analysis of the kinetic results in terms of these electrostatic interactions reveals the overall protein-protein orientation for electron transfer. In both the forward and back reactions the exposed heme edge in zinc cytochrome *c* apparently abuts the negatively-charged (acidic) patch on the plastocyanin surface, which is remote from the copper atom, and not the electroneutral (hydrophobic) patch, which is proximate to the copper atom. The acidic patch is large, and this analysis cannot rule out a relatively small difference in protein–protein orientations for the forward and back reactions. These two reactions are compared with the previously studied reduction of cupriplastocyanin by ferrocytochrome *c*. Although native cytochrome *c* and its zinc derivative have very similar structural and electrostatic properties, the reactive forms of the cytochrome *c*/plastocyanin and zinc cytochrome *c*/plastocyanin complexes may adopt somewhat different protein–protein orientations or may adopt similar orientations but differ in dynamic properties.

Respiratory and photosynthetic electron-transport chains are highly directional because redox reactions of metalloproteins and of other redox agents are highly selective (Hoffman et al., 1991; McLendon, 1991a,b; Therien et al., 1991; Beratan et al., 1991; Mauk, 1991; Kostić, 1991; Winkler & Gray, 1992; McLendon & Hake, 1992). To understand molecular basis of this selectivity, one must understand protein–protein interactions that determine donor–acceptor distance and orientation. Since charged groups in most proteins are asymmetrically distributed, electrostatic interactions can be very anisotropic. Analysis of this anisotropy by kinetic methods can reveal protein–protein orientation in the electron-transfer reaction.

The heme protein cytochrome *c* (Pettigrew & Moore, 1987; Moore & Pettigrew, 1990) and the blue copper protein plastocyanin (Sykes, 1991a,b), which are designated cyt and pc,[1] are well suited to studies of donor–acceptor orientation. Their three-dimensional structures are known in detail, their properties have been thoroughly examined by spectroscopic and electrochemical methods, and mechanisms of their redox reactions with many agents have been studied by various kinetic methods. The physiological partner of plastocyanin is cytochrome *f*, which resembles cytochrome *c* in several regards (Qin & Kostić, 1992, 1993). Cytochrome *f*, however, cannot be used in these studies of protein–protein orientation because its three-dimensional structure is unknown.

Plastocyanin is notable among small metalloproteins for it contains two distinct surface patches through which it can exchange electrons with redox partners. The negatively charged acidic patch is remote (14–19 Å) from the copper atom, while the electroneutral hydrophobic patch is proximate (3–9 Å) to this atom. (Different amino acid residues in each patch correspond to different distances from the copper atom.) The rate of electron transfer through proteins may be controlled by the donor–acceptor distance (Moser et al., 1992), or specific paths through bonds may exist (Beratan et al., 1991; Wuttke et al., 1992; Betts et al., 1992). From either of these current points of view, plastocyanin possesses at least two channels, through the two surface patches, for electron transfer to and from the buried copper site. The choice between the two channels, and therefore between the two patches, is often attributed simply to the charge of the other reactant (Sykes, 1991a,b). A recent theoretical analysis of paths through bonds indicated that the barrel structure of plastocyanin provides relatively strong electronic coupling of the copper atom to the strands to which it is ligated but not to other strands. Both of the aforementioned patches consist of the side chains in the ligated strands (Betts et al., 1992). Another theoretical analysis, by a different method, distinguished these two channels. The channel via the hydrophobic patch seems to provide stronger electronic coupling, but the one via the acidic patch is enhanced by the possibility of electrostatic binding of the positively-charged redox agent to the protein surface (Christensen et al., 1990).

In cytochrome *c* the exposed heme edge is surrounded by lysine residues. Since this positively-charged (basic) patch is considered the only surface site for electron transfer to and from the heme group, cytochrome *c* is ideally suited for probing

† N.M.K. thanks the National Science Foundation for a Presidential Young Investigator Award (Grant CHE-8858387) and the A. P. Sloan Foundation for a Research Fellowship for 1991–93, which supported this work.

[1] Abbreviations: CM, center of mass; cyt, cytochrome *c*; cyt(II), ferrocytochrome *c*; cyt(III), ferricytochrome *c*; EDC, 1-ethyl-3-[3-(dimethylamino)propyl]carbodiimide hydrochloride; NHE, normal hydrogen electrode; pc, plastocyanin; pc(I), cuproplastocyanin; pc(II), cupriplastocyanin; Zncyt, zinc cytochrome *c*; $^3$Zncyt, triplet state of zinc cytochrome *c*; Zncyt$^+$, zinc cytochrome *c* cation radical.

0006-2960/93/0432-4539$04.00/0 

the surface of plastocyanin. Replacement of iron(II) by zinc(II) does not perturb the conformation of cytochrome *c* and its association with other proteins (Moore et al., 1980; Vanderkooi & Erecinska, 1975; Vanderkooi et al., 1976). While native ferrocytochrome *c* is a weak reductant ($E°$ = 0.26 V vs NHE), the triplet state of its zinc derivative is a strong one ($E°$ = –0.88 V) (Magner & McLendon, 1989); cupriplastocyanin ($E°$ = 0.36 V) can oxidize both of them. (All these three numbers are reduction potentials at pH 7.0.)

Ferrocytochrome *c* and cupriplastocyanin have overall charges of +6 and –8 at pH 7.0, and they contain oppositely charged patches on their surfaces. For both of these reasons, these two proteins form a complex in solution at low ionic strength. Much evidence shows that in the complexes cyt/pc and Zncyt/pc the positive patch around the exposed heme edge abuts an area within the broad negative patch in plastocyanin (Augustin et al., 1983; Armstrong et al., 1986; Anderson et al., 1987; Burkey & Gross, 1981, 1982; Chapman et al., 1984; Geren et al., 1983; King et al., 1985; Bagby et al., 1990; Roberts et al., 1991). This configuration is noninvasively reinforced by covalent cross-linking in the presence of the carbodiimide designated EDC (Green et al., 1983; Peerey & Kostić, 1989; Peerey et al., 1991; Zhou et al., 1992).

The protein molecules, however, need not react with each other in the same orientation in which they dock with each other. This notion is nicely illustrated by cytochrome *c* and plastocyanin. Study by others of the bimolecular reaction in eq 1 (Modi et al., 1992a,b) and study in this laboratory of the unimolecular electron-transfer step (eq 2) in this reaction

$$\text{cyt(II)} + \text{pc(II)} \rightarrow \text{cyt(III)} + \text{pc(I)} \quad (1)$$

$$\text{cyt(II)/pc(II)} \rightarrow \text{cyt(III)/pc(I)} \quad (2)$$

(Peerey & Kostić, 1989; Peerey et al., 1991), taken together, showed that ferrocytochrome *c* does reduce cupriplastocyanin from the acidic patch but not from the initial binding site within this broad patch. Our preliminary study of the reactions in eqs 3 (Zhou & Kostić, 1991b) and 4 (Zhou & Kostić,

$$^3\text{Zncyt} + \text{pc(II)} \xrightarrow{k_f} \text{Zncyt}^+ + \text{pc(I)} \quad (3)$$

$$^3\text{Zncyt/pc(II)} \rightarrow \text{Zncyt}^+\text{/pc(I)} \quad (4)$$

1992a) indicated that zinc cytochrome *c* in the triplet state can reduce cupriplastocyanin from the initial binding site within the acidic patch. In this full report we examine in detail the protein–protein orientation in the photoinduced "forward" reaction (eq 3) and in the thermal "back" reaction (eq 5); the unimolecular counterpart of the latter reaction is shown in eq 6. Our first goal is to compare the two bimolecular

$$\text{Zncyt}^+ + \text{pc(I)} \xrightarrow{k_b} \text{Zncyt} + \text{pc(II)} \quad (5)$$

$$\text{Zncyt}^+\text{/pc(I)} \rightarrow \text{Zncyt/pc(II)} \quad (6)$$

reactions and find out whether protein–protein orientation depends on the factors in which these reactions differ, namely, the thermodynamic driving force (1.2 eV in eq 3 vs 0.44 eV in eq 5) and the direction of electron transfer (reduction vs oxidation of plastocyanin). Our second goal is to analyze electrostatic interactions between zinc cytochrome *c* and plastocyanin and to compare critically three theoretical models of these interactions.

## MATERIALS AND METHODS

*Chemicals.* Horse heart cytochrome *c* (Type III) was obtained from Sigma Chemical Co. Iron was removed, the free-base protein was purified, and zinc was inserted according to published procedures, in the dark. Zinc cytochrome *c*, Zncyt, was always handled in the dark (Vanderkooi & Erecinska, 1975; Vanderkooi et al., 1976). French-bean plastocyanin was isolated by standard methods (Milne & Wells, 1970) and purified repeatedly by gel-filtration chromatography on Sephadex G-25 and G-75 columns and by anion-exchange chromatography on a Sephadex DEAE A-25 column until the absorbance quotient $A_{278}/A_{597}$ became less than 1.20. Cuproplastocyanin, pc(I), was always prepared fresh by reduction of the protein by ascorbic acid and by removal of the reductant and of other small molecules by a Bio-Gel P-6 column. Concentration of cuproplastocyanin in stock solutions was determined by oxidizing an aliquot with an excess of $K_3[Fe(CN)_6]$ and by measuring the absorbance of the resulting cupriplastocyanin, pc(II), whose absorptivity at 597 nm is 4500 $M^{-1}$ $cm^{-1}$. Oxidation of cuproplastocyanin by air was not detected.

Distilled water was further purified by the Barnstead Nanopure II apparatus. Potassium phosphate buffer was prepared with salts of molecular biology reagent grade, obtained from Sigma Chemical Co. It had a pH of 7.0 and an ionic strength of 10 mM; higher ionic strengths were achieved by addition of NaCl.

*Kinetics.* Laser kinetic spectroscopy (so-called laser flash photolysis) on the microsecond scale was done with a standard apparatus (Zhou & Kostić, 1991a,b, 1992a,b). The sample solution in a 10-mm cuvette was throughly deaerated by gentle flushing with ultrapure argon supplied by Air Product Co. Ionic strength of the phosphate buffer at pH 7.0 was varied from 40 mM to 3.00 M. A Phase-R DL1100 laser contained a 50 $\mu$M solution of rhodamine 590 in methanol and delivered 0.4-$\mu$s pulses of excitation light. The monitoring beam from a tungsten–halogen lamp (source Oriel 60065) passed through the filter monochromator Oriel 7155 and was perpendicular to the excitation beam. All the lenses were achromatic, with a coating that minimized surface reflectance. A grating monochromator Oriel 77250 was placed before the photomultiplier tube Hamamatsu R928. The F numbers and other characteristics of the optical parts were matched for maximum throughput. The absorbance–time curves were obtained and analyzed with kinetic software from OLIS, Inc. Decay of the triplet state of zinc cytochrome *c*, designated $^3$Zncyt, was monitored at 460 nm, where this transient absorbance reaches a maximum. After each laser pulse 500 data points were collected, and each signal was an average of six pulses. Kinetic data over at least three half-lives after the laser pulse were used in the fittings. Formation and decay of the cation radical, designated $Zncyt^+$, were monitored at 675 nm, where the difference in absorbance between the cation radical and the triplet state is greatest. Again, after each laser pulse 500 data points were collected, but now each signal was an average of 20 pulses. Kinetic data were fitted in two ways—successive integration (SI-FIT) and the Levenberg–Marquardt nonlinear algorithm gave consistent results. Fittings over different time intervals gave rate constants that differed only within the error bounds. The back reaction (eq 5) was either analyzed in terms of sequential first-order processes or the very few data points corresponding to an initial increase in absorbance were ignored; the two methods gave consistent results. The sample cuvette was thermostated at 25.0 ± 0.2 °C.

The concentration of zinc cytochrome *c* was always 10.0 $\mu$M. The concentrations of the triplet $^3$Zncyt and of the cation

radical Zncyt$^+$ depended on the excitation power. In the study of the forward reaction (eq 3) the triplet concentration was 0.30–1.0 $\mu$M and was always less than $^1/_{10}$ the concentration of the quencher, cupriplastocyanin, which was varied from 5.0 to 30 $\mu$M. The forward reaction was studied in the absence and in the presence of added cuproplastocyanin.

In the study of the back reaction (eq 5) the concentration of the cation radical was 0.1–0.3 $\mu$M, and was always less than $^1/_{20}$ the concentration of added cuproplastocyanin, which was varied from 2.0 to 8.0 $\mu$M. Cuproplastocyanin formed in the forward reaction added negligibly little to the 20-fold excess over Zncyt$^+$ and was not taken into account. The concentration of cupriplastocyanin was 6–8 times higher than that of cuproplastocyanin. At high ionic strength, concentration of cupriplastocyanin was raised up to 60 $\mu$M in order to keep the forward reaction fast and well separated in time from the back reaction.

As these experimental details show, both reactions were studied under conditions of kinetic pseudo-first-order. Second-order rate constants at different ionic strengths were obtained from the corresponding pseudo-first-order rate constants by least-squares fittings. Each pseudo-first-order rate constant is an average result from two or three experiments, but error bars are not shown in the plots of the rate constants versus the plastocyanin concentration. Since the rate constants in the absence of plastocyanin are determined by actual experiments, the intercepts were fixed in these fittings. This procedure and analysis in terms of parallel first-order processes gave consistent results.

*Calculations of Dipole Moments.* Atomic coordinates for horse heart cytochrome *c* were obtained from its crystal structure (Bushnell et al., 1990). Atomic coordinates for French-bean plastocyanin were obtained from the crystal structure of the poplar protein (Guss & Freeman, 1983) by replacing the relatively few nonhomologous amino acid residues. Partial charges were assigned to all atoms (McCammon et al., 1979; Northrup et al., 1981). The net charge and magnitude and orientation of the dipole moment in all cases were calculated by an established method (Koppenol & Margoliash, 1982; Northrup et al., 1986). The iron(II) ion was replaced by a zinc(II) ion, and the oxidation state of copper was set at both I and II. It was reasonably assumed that at pH 7.0 all lysine and arginine side chains are protonated, that the terminal amino group is protonated in plastocyanin but not in cytochrome *c*, and that the sulfhydryl group coordinated to the copper atom and all carboxylic groups are deprotonated.

*Treatments of Electrostatic Interactions.* The most widely used theoretical treatment is based on transition-state formalism. According to it, the rate constant depends on ionic strength because activity coefficients of the reactants and of the transition state depend on it (Glasstone et al., 1940). Description of this dependence in terms of Debye–Hückel theory yields eq 7. The symbols in this and following equations

$$\ln k = \ln k_0 - \frac{Z_1^2\alpha\sqrt{\mu}}{1+\kappa R_1} - \frac{Z_2^2\alpha\sqrt{\mu}}{1+\kappa R_2} + \frac{(Z_1+Z_2)^2\alpha\sqrt{\mu}}{1+\kappa R_\ddagger} \quad (7)$$

have the following meanings: $k$ and $k_0$, respectively, are bimolecular rate constants at ionic strengths $\mu$ and zero; $Z_1$ and $Z_2$ are net charges and $R_1$ and $R_2$ are radii of the reactants; $R_\ddagger$ is the radius of the transition state for the bimolecular reactions, which can be equated with the radius of the electrostatic complex cyt/pc, estimated at 20.6 Å by two independent methods (Zhou & Kostić, 1992b; Brothers et al., 1993); $\alpha$ = 1.17 in water at 25 °C; and $\kappa = 0.329\sqrt{\mu}$ Å$^{-1}$.


FIGURE 1: Chain of $\alpha$ carbon atoms (Bushell et al., 1990) and calculated dipole vector of ferrocytochrome *c*. The numerals represent selected amino acid residues, and angles $\theta_2$ define positions with respect to the positive end of the dipole vector.

Under the assumption $R_1 = R_2 = R_{av}$, eq 7 reduces to the well-known eq 8, which is tested in this study. The radii of

$$\ln k = \ln k_0 + \frac{2Z_1Z_2\alpha\sqrt{\mu}}{1+\kappa R_{av}} \quad (8)$$

cytochrome *c* and of plastocyanin are 18.5 and 15.5 Å, respectively. We follow investigators of the reaction in eq 1 (Rush et al., 1988) in setting the average radius $R_{av}$ at 18.5 Å.

In eq 9, which is based on the Marcus theory of electron transfer (Wherland & Gray, 1977), $k_\infty$ is the rate constant at infinite ionic strength, and $D$ is the distance between the two redox sites; it is estimated at 20 Å (Augustin et al., 1983).

$$\ln k = \ln k_\infty - 3.576\left(\frac{\exp(-\kappa R_2)}{1+\kappa R_1} + \frac{\exp(-\kappa R_1)}{1+\kappa R_2}\right)\frac{Z_1Z_2}{D} \quad (9)$$

$$\ln k = \ln k_\infty - [Z_1Z_2 + Z\mathbf{P}(1+\kappa R) + \mathbf{PP}(1+\kappa R)^2]\frac{e^2}{4\pi\epsilon_0\epsilon k_B T R^4} f(\kappa) \quad (10)$$

The theory embodied in eq 10 recognizes not only net charges ($Z$) but also dipole moments (vectors **P** with magnitudes $P$) of the protein molecules (van Leeuwen et al., 1981; van Leeuwen, 1983; Rush et al., 1987, 1988). The monopole–dipole (eq 11) and dipole–dipole (eq 12) interactions are

$$Z\mathbf{P} = \frac{Z_1P_2\cos\theta_2 + Z_2P_1\cos\theta_1}{eR} \quad (11)$$

$$\mathbf{PP} = \frac{P_1P_2\cos\theta_1\cos\theta_2}{(eR)^2} \quad (12)$$

anisotropic—they depend on the location of the surface docking sites with respect to the dipole vectors. The function of ionic strength is defined in eq 13. The new symbols in eqs 9–13

$$f(\kappa) = \frac{1-\exp(-2\kappa R)}{2\kappa R_2(1+\kappa R_1)} \quad (13)$$

have the following meanings: $\theta$ is the angle between the dipole vector and the vector from the center of mass (CM) to the reaction site on the surface (see Figures 1 and 2), $R = R_1 +$

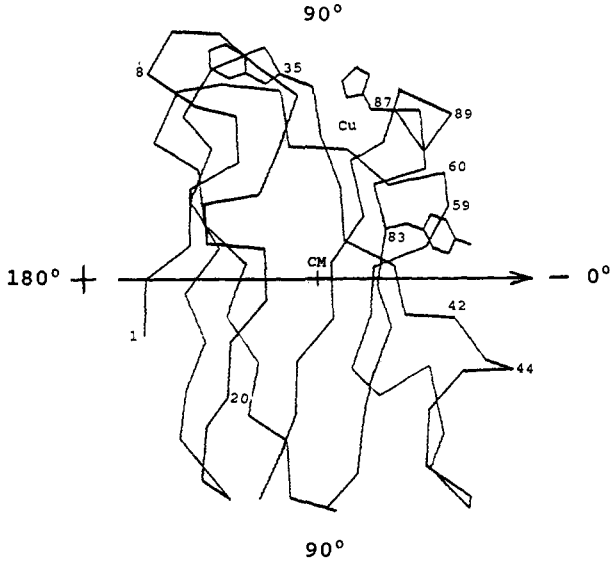


FIGURE 2: Chain of $\alpha$ carbon atoms (Guss & Freeman, 1983) and calculated dipole vector of cupriplastocyanin. The numerals represent selected amino acid residues, and angles $\theta_1$ (see Table II) define positions with respect to the negative end of the dipole vector.

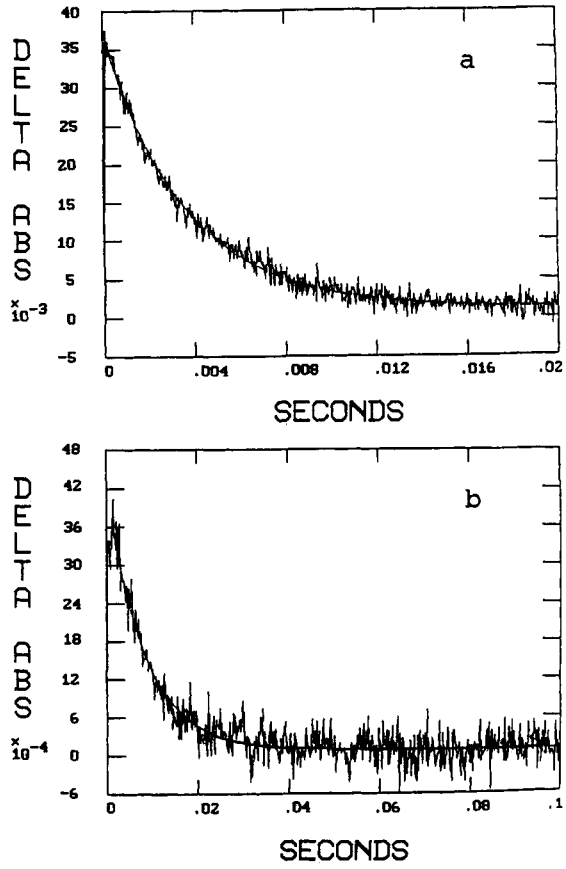


FIGURE 3: Transient absorbance changes in a solution containing 10.0 $\mu$M zinc cytochrome *c*, 60.0 $\mu$M cupriplastocyanin, and 8.0 $\mu$M cuproplastocyanin in phosphate buffer at pH 7.0, ionic strength of 3.00 M, and 25 °C. Each solid line is a single-exponential fitting. The time scales are chosen to show both curved and linear portions of the traces. (a) The triplet state, $^3$Zncyt, monitored at 460 nm. (b) The cation radical, Zncyt$^+$, monitored at 675 nm, disappears by a process of pseudo-first-order. The fitting (solid line) begins at 5 ms.

$R_2$, $\epsilon_0$ is the permittivity constant, $\epsilon$ is the static dielectric constant, $k_B$ is the Boltzmann constant, and $e$ is elementary charge.

In eqs 7–13, subscript 1 ($Z_1$, $P_1$, and $\theta_1$) designates plastocyanin, and subscript 2 ($Z_2$, $P_2$, and $\theta_2$) designates zinc cytochrome *c*. Estimated uncertainty in $\theta$ is the interval of its values over which the average difference between the best fitted and the experimentally determined values of $k$ at all ionic strengths is 10% or less.

Table I: Dependence on Ionic Strength of the Rate Constant for Bimolecular Reactions at pH 7.0 and 25 °C

| rate constant ($\times 10^{-7}$ M$^{-1}$ s$^{-1}$)[a] | $\mu$ (mM) | | | | | | | | |
|---|---|---|---|---|---|---|---|---|---|
| | 40 | 50 | 60 | 80 | 100 | 200 | 500 | 1000 | 3000 |
| $k_f$ (eq 3) | 70 | 31 | 23 | 15 | 13 | 4.0 | 1.4 | 0.94 | 0.67 |
| $k_b$ (eq 5) | 127 | 90 | 51 | 27 | 18 | 5.9 | 2.0 | 1.4 | 1.1 |

[a] Estimated error, ±10%.

## RESULTS

*Decay of $^3$Zncyt.* The triplet excited state decayed exponentially, with the rate constant of 100 ± 10 s$^{-1}$, in the entire range of ionic strength from 40 mM to 3.00 M. This rate constant remained unchanged in the presence of 10.0 $\mu$M cuproplastocyanin.

*Forward Reaction between $^3$Zncyt and Cupriplastocyanin.* In the presence of cupriplastocyanin decay of the triplet state became faster but remained exponential at all ionic strenths; see Figure 3a. The rate constants for disappearance of $^3$Zncyt and for appearance of Zncyt$^+$ were equal within the error bounds. The cation radical disappeared in a second-order process. The pseudo-first-order rate constant was linearly proportional to the cupriplastocyanin concentration at all ionic strengths, and it varied with ionic strength. Bimolecular rate constants, calculated from the slopes of the linear plots in Figure 1 in the supplementary material, are given in Table I.

*Back Reaction between Zncyt$^+$ and Cuproplastocyanin.* Addition of cuproplastocyanin did not alter the rate of quenching of $^3$Zncyt by cupriplastocyanin, but it made the disappearance of Zncyt$^+$ an exponential process of pseudo-first-order; see Figure 3b. The pseudo-first-order rate constant was linearly proportional to the cuproplastocyanin concentration at all ionic strengths, and it varied with ionic strength. Bimolecular rate constants, calculated from the slopes of the linear plots in Figure 4, are given in Table I.

*Dipole Moments.* Our calculation for horse heart ferrocytochrome *c*, whose net charge is +6, reproduced the value of 281 D obtained previously (Northrup et al., 1986). As Figure 1 shows, the dipole vector forms an angle of 30° with the vector from the center of mass to the iron atom. The positive end of the vector penetrates the surface near the carbonyl carbon atom of Ile 81, and the negative end penetrates it near the $\delta_2$ carbon atom of Phe 36. The exposed heme edge is located at 20–40° with respect to the positive end of the dipole vector. Very similar results were obtained by different calculational methods (Koppenol et al., 1991). Properties of French-bean cupriplastocyanin and cuproplastocyanin, respectively, are as follows: net charge, –8 and –9; effective radius, 15.5 Å for both; dipole moment, 362 and 370 D; angle between the dipole vector and the vector from the center of mass to the copper atom, 80° and 72°; atoms near which the positive end of the dipole vector penetrates the protein surface, $\alpha$ carbon of Glu 2 and nitrogen of Glu 2; and atoms near which the negative end of the dipole vector penetrates the protein surface, oxygen of Val 41 and hydroxyl oxygen of Tyr 83. See Figure 2. The locations of the hydrophobic and acidic patches with respect to the dipole vector are given in Table II.

## DISCUSSION

*Nonredox Quenching of $^3$Zncyt.* Our rate constant of 100 ± 10 s$^{-1}$ for the natural decay of the triplet state of zinc

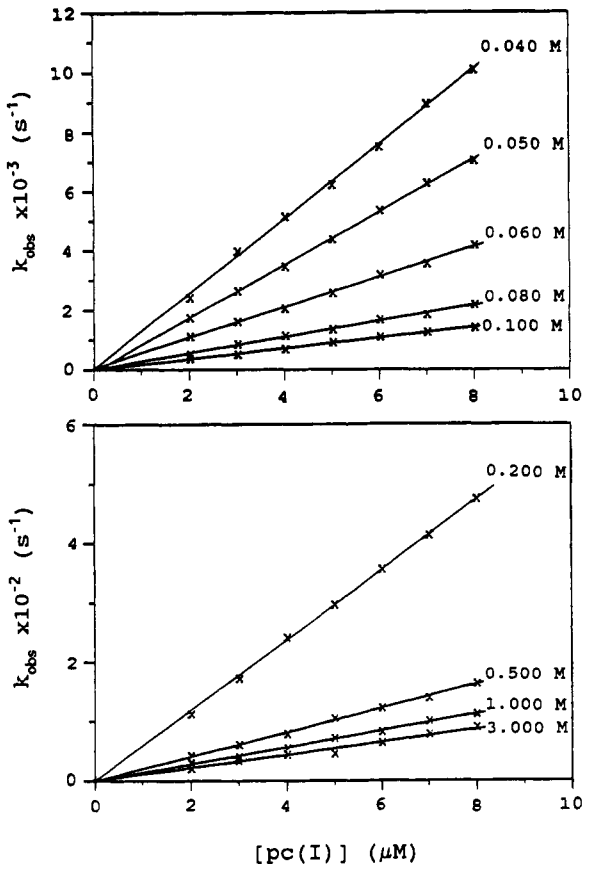


FIGURE 4: Rate of disappearance of the cation radical, Zncyt$^+$, as a function of cuproplastocyanin concentration in phosphate buffer at the indicated ionic strength (molar), pH 7.0, and 25 °C. Solid lines are linear least-squares fittings.

Table II: Orientations of Selected Sites in French-Bean Plastocyanin with Respect to the Negative End of the Dipole Vector

| patch | site | $\theta_1$ (deg) pc(I) | $\theta_1$ (deg) pc(II) |
|---|---|---|---|
| | Cu | 72 | 80 |
| hydrophobic | His 87, imidazole | 67–73 | 73–80 |
| | Phe 35, phenyl | 97–106 | 107–110 |
| | Pro 36, $\alpha$-C | 81 | 87 |
| acidic | Tyr 83, ring | 3–23 | 10–28 |
| | cluster 42–45 | 25–47 | 18–42 |
| | cluster 59–61 | 22–60 | 25–60 |

cytochrome *c* falls in the middle of a narrow range, 70–140 s$^{-1}$, spanned by the values reported before (Elias et al., 1988; Vos et al., 1987; Dixit et al., 1981, 1984; Horie et al., 1985). The slight variation in the rate constant perhaps is caused by small differences in the protein preparation, deoxygenation procedure, buffer, and temperature. This variation does not affect the following kinetic arguments and conclusions. The decay rate (i.e., the lifetime) of the triplet state is unaffected by the presence of cuproplastocyanin. Although the triplet state in principle can both donate ($E^\circ = -0.88$ V) and accept ($E^\circ \approx 0.4$ V) electrons, reductive bimolecular quenching (eq 14) cannot compete with the natural decay.

$$^3\text{Zncyt} + \text{pc(I)} \rightarrow \text{Zncyt}^- + \text{pc(II)} \qquad (14)$$

*Forward Electron-Transfer Reaction.* Our previous study (Zhou & Kostić, 1991a) showed that quenching of $^3$Zncyt by cupriplastocyanin is due to the electron-transfer reaction in eq 3 and not to energy transfer, association with the quencher, and other nonredox processes. Since the plots in Figure 1 in the supplementary material are linear, quenching is purely bimolecular at ionic strengths of 40 mM and greater. Since the decay is monoexponential, zinc cytochrome *c* does not associate with cupriplastocyanin to a significant extent at ionic strengths of 40 mM and greater. The association constant is approximately $5 \times 10^3$ M$^{-1}$ at the ionic strength of 40 mM. At lower ionic strengths the decay of $^3$Zncyt becomes biexponential because the electrostatic complex Zncyt/pc(II) already exists before the laser flash (Zhou & Kostić, 1991a).

Added cuproplastocyanin, in the presence of a 6–8-fold excess of cupriplastocyanin, does not affect the redox quenching in eq 3. Therefore the ratio of association constants for formation of the precursor complexes Zncyt/pc(I) and Zncyt/pc(II) cannot be greater than 2:1. If cuproplastocyanin, which bears a greater negative charge, formed a significantly more stable complex, addition of this protein would inhibit redox quenching. It does not.

*Back Electron-Transfer Reaction.* As the time axes in Figure 3 show, the reaction in eq 3 takes place in a shorter time than the subsequent reaction in eq 5. This separation was achieved by using a relatively high concentration of cupriplastocyanin, so that kinetic analysis of the back reaction is straightforward. Since the plots in Figure 4 are linear, this reaction too is purely bimolecular at ionic strengths of 40 mM and greater.

*Dependence of Rate Constants on Ionic Strength.* As Figure 1 in the supplementary material, Figure 4, and Table I show, both reactions in eqs 3 and 5 between oppositely-charged proteins are greatly assisted by decreasing ionic strength, as expected. At a given ionic strength $k_b$ is greater than $k_f$, in part because the charges of the proteins in the back reaction differ more (they are greater by one unit each) than the charges of the proteins in the forward reaction. But this cannot be the whole explanation because the rate constants remain different even at the ionic strength of 3.00 M, at which electrostatic interactions are insignificant.

*Monopole–Monopole Electrostatic Interactions.* Fittings of the kinetic results in Table I to eq 7 are shown in Figure 5a. When the correct net charges $Z_1$ and $Z_2$ of the protein molecules are used, fitting requires unreasonable values of the rate constant $k_0$, which are far too large even for a diffusion-controlled reaction between oppositely charged proteins (Eigen & Hammes, 1963). When the correct charge $Z_1$ of plastocyanin (–8 for the forward reaction and –9 for the back reaction) is used and both $k_0$ and $Z_2$ are allowed to vary, the best fittings to eq 7 gave reasonable values of the former variable but too low values of the latter one: $k_0 = 9.7 \times 10^{10}$ M$^{-1}$ s$^{-1}$ and $Z_2 = 2.7$ for the forward reaction and $k_0 = 2.2 \times 10^{11}$ M$^{-1}$ s$^{-1}$ and $Z_2 = 2.3$ for the back reaction. The correct values of $Z_2$ are 6 and 7, respectively. Debye–Hückel treatment evidently is inapplicable.

Application of eq 8 at ionic strengths of 40–200 mM gave the charge products of –42 and –52 for the forward and back reactions, respectively. These values are incorrect, probably because of the simplifying assumption about the radii, used in deriving eq 8 from eq 7, and because Debye–Hückel theory is fully valid only at low ionic strengths (Marcus & Sutin, 1985). But the calculated charge products do not deviate greatly from the expected ones, which are –48 and –63. Since errors of this magnitude may be tolerable in some applications, Debye–Hückel theory and various approximations to it remain useful for qualitative analysis of electrostatic interactions between proteins.

Fittings of the kinetic results in Table I to eq 9 are shown in Figure 5b. This treatment, too, fails at ionic strengths greater than ca. 200 mM. Its application at ionic strengths of 40–200 mM gave the grossly incorrect charge products of

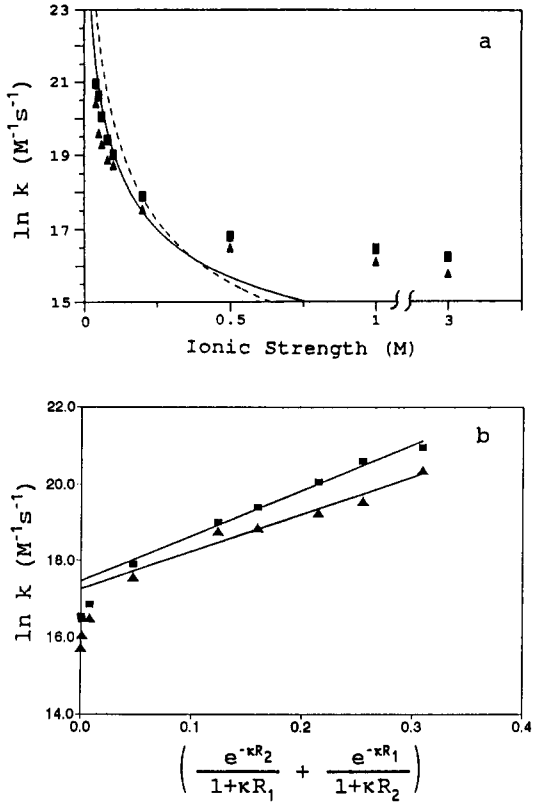


FIGURE 5: Dependence on ionic strength (40, 50, 60, 80, 100, 200, 500, 1000, and 3000 mM) of the bimolecular rate constants for the reactions in eqs 3 (▲) and 5 (■) in phosphate buffer at pH 7.0 and 25 °C. (a) The solid line is the fitting to eq 7 of the reaction in eq 3 with the known parameters $Z_1 = -8$ and $Z_2 = 6$ fixed and with the unreasonable variable parameter $k_0 = 9.6 \times 10^{13}$ $M^{-1}$ $s^{-1}$. The dashed line is the fitting to eq 7 of the reaction in eq 5 with the known parameters $Z_1 = -9$ and $Z_2 = 7$ fixed and with the unreasonable variable parameter $k_0 = 1.3 \times 10^{16}$ $M^{-1}$ $s^{-1}$. Note the break in the horizontal scale. (b) Solid lines are fittings to eq 9 over the range 40–200 mM.

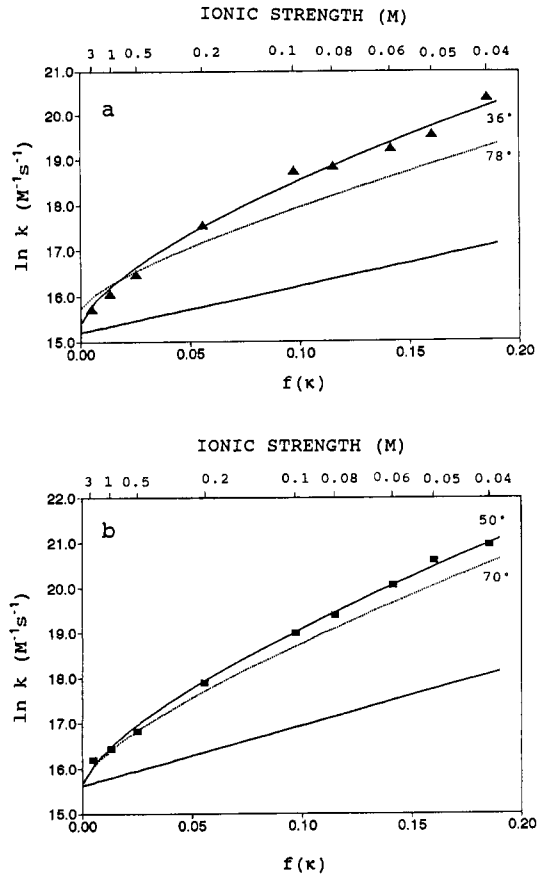


FIGURE 6: Dependence on ionic strength at pH 7.0 and 25 °C of the bimolecular rate constants for the reactions in eq 3 (a) and eq 5 (b). The solid curves are fittings to the complete eq 10, and the best values of the angle $\theta_1$ are shown. The dotted curves are obtained from the complete eq 10 with the angle $\theta_1$ fixed at the value for His 87 at the hydrophobic patch. The solid straight lines are obtained from eq 10 by neglect of monopole–dipole and dipole–dipole interactions. Note that the horizontal axis is marked in two different ways.

−158 and −192 for the forward and back reactions, respectively. Correct charge products could be obtained only by using an impossibly long distance $D$. Even more serious than these quantitative discrepancies is the great qualitative deviation of the experimental results from the linear dependence embodied in eq 9. Neither of these theories satisfactorily describes variation of the rate constants over the entire range of ionic strength.

*Monopole–Dipole and Dipole–Dipole Interactions and the Protein Orientation for Electron Transfer.* Since the three-dimensional structures of both cuprous and cupric forms of plastocyanin are known in detail, we calculated the dipole moments for both of them. The magnitude and orientation of the vectors differ only slightly because the protein structure changes very little with the change of the copper oxidation state. We had to use the dipole moment of ferrocytochrome *c* for zinc cytochrome *c* and for its cation radical. Although the three-dimensional structures of the last two species are unknown, it is known that replacement of iron(II) by zinc(II) does not noticeably change the protein structure and topography (Vanderkooi & Erecinska, 1975; Vanderkooi et al., 1976; Moore et al., 1980). Any errors caused by this approximation and by the unavoidable neglect of the delocalization of the porphyrin charge in the cation radical $Zncyt^+$ probably are small; they are kept in mind in determining the liberal error bounds of the angle $\theta_1$ (fittings to eq 10) and in the analysis of dipolar interactions in terms of protein–protein orientation.

Dipolar interactions are an important component of the total electrostatic interaction between protein molecules having asymmetric charge distributions. Dipolar interactions manifest themselves especially clearly when the reactants have large dipole moments and at least one of them has only small net charge, so that the monopole–monopole interaction is weak. In such cases dependence of the rate constant on ionic strength is mostly caused by dipolar interactions (Zhou & Kostić, 1992b; Brothers et al., 1993). These previous experiments and the present successful fittings to eq 10 of rate constants at high as well as low ionic strengths validate the following analysis.

The fittings are shown in Figure 6. The straight lines in both cases are obtained by neglecting dipolar interactions; complete divergence of these lines from the data points demonstrates the importance of these interactions.

Since cytochrome *c* undergoes electron transfer via the exposed heme edge, which forms an angle of 30° with the dipole vector, this value of the fixed parameter $\theta_2$ is justified a priori; it is not used to improve the fittings. The fixed parameters $Z_1$ and $Z_2$ are known exactly, from the structures of the two proteins. The two variable parameters in the fittings are $k_\infty$ and $\theta_1$. The $k_\infty$ values for the forward (eq 3) and back (eq 5) reactions are $(1.3 \pm 0.3) \times 10^6$ and $(2.0 \pm 0.4) \times 10^6$ $M^{-1}$ $s^{-1}$, respectively. These values at infinite ionic strength are reasonable because they continue the trends in Table I. The forward rate constants at ionic strengths from 40 to 100 mM could be made to fit eq 10 with the fixed angle $\theta_1$ of 78° only if $k_\infty$ is set at $1.7 \times 10^7$ $M^{-1}$ $s^{-1}$, a value that badly deviates

from the experimental results in Table I; it is larger than the experimental value at the ionic strength of 500 mM. This discrepancy alone may not be the compelling reason for rejection of the fit with 78° because eq 10 is not expected to apply strictly at high ionic strength and because nonelectrostatic (primarily hydrophobic) interactions between the protein molecules at high ionic strength cannot be ruled out. Our previous study (Zhou & Kostić, 1991a), however, showed that these interactions are far less important than electrostatic ones in determining protein–protein interactions. The electrostatic theory embodied in eq 10 proved applicable to ionic strengths greater than 100 mM in many (Zhou & Kostić, 1991b, 1992b; Brothers et al., 1993; Rush et al., 1988; Dixon et al., 1989, 1990; Dixon & Hong, 1990) but not all (Eltis et al., 1991) studies of diprotein systems. Even in this last report, however, such applications were judged acceptable. For these reasons, we believe that the solid and dotted curves in Figure 6a are indeed different and that only the former one satisfactorily fits the experimental points.

The following discussion will be based on the analysis of electrostatic interactions. Although a $\theta_1$ value defines a band, not a particular spot, on the plastocyanin surface, this value allows a distinction between distant areas on the protein surface. The angles $\theta_1$ for the forward and back reactions are 36° ± 15° and 50° ± 10°, respectively. These values are inconsistent with the hydrophobic patch in either cupriplastocyanin or cuproplastocyanin, as Table II and the dotted lines in Figure 6 show. These values of $\theta_1$ are consistent with the acidic patch in both oxidized and reduced forms of plastocyanin. Since the two $\theta_1$ values are equal within the error bounds, and since the theory embodied in eq 10 is semiquantitative (Eltis et al., 1991), an attempt to pinpoint particular sites within the broad acidic patch and more precisely to define the protein–protein orientation on the basis of these kinetic fittings would be unwarranted.

In a previous study of the unimolecular reaction in eq 4 we found that orientations for initial docking and for electron transfer are probably different although both of them involve the broad acidic patch in plastocyanin (Zhou & Kostić, 1992a). The fitting in Figure 6a, discussed above, is consistent with the involvement of this patch. In this study of bimolecular reactions we can only conclude that plastocyanin apposes its acidic patch to the protruding heme edge both when it is reduced by $^3$Zncyt (eq 3) with a driving force of 1.2 eV and when it is oxidized by Zncyt$^+$ (eq 5) with a driving force of 0.44 eV. The values of 36° and 50° may be considered equal because of the approximations embodied in eq 10 and because of the cautions way in which we set the error bounds. Nonetheless, the nominal difference between these two values of $\theta_1$ may reflect an actual small difference in the protein–protein orientations for the forward and back reactions.

*Comparisons with the Reaction between Plastocyanin and Native Cytochrome c.* Analysis of dipolar interactions (Rush et al., 1988) indicated that cupriplastocyanin does not use its acidic patch, and that it perhaps uses its hydrophobic patch, in the reaction with ferrocytochrome *c* (eq 1). Effects of site-directed mutagenesis in plastocyanin on kinetics of the reaction in eq 1, however, showed that cupriplastocyanin does use its acidic patch for this reaction. In the pictorial Scheme I, patches on the surfaces of both proteins are represented with circles (for amino acid residues), the charges of the charged patches are shown, and the exposed heme edge is highlighted. This scheme shows the unimolecular electron-transfer step (eqs 2, 4, and 6) in each bimolecular reaction (eqs 1, 3, and 5, respectively). Although native cytochrome *c* and its zinc derivative (in the triplet state and as the cation radical) have similar topographies and electrostatic properties, reactive protein–protein orientation may be governed not only by docking interactions but also by other factors. The contrast between the reaction in eq 1 on the one side and the reactions in eqs 3 and 5 on the other may perhaps be attributed to a difference in the thermodynamic driving force for these reactions: small (0.10 eV for eq 1) on the one side versus large (1.2 eV for eq 3) and intermediate (0.44 eV for eq 5) on the other. When the driving force is small, conformational fluctuations at the interface between the acidic patch and the exposed heme edge are needed to optimize electron-transfer paths, or to minimize the heme–copper distance, or both. This case is shown in the upper part of Scheme I. When, however, the driving force is intermediate or large, an electron can be transferred from the initial docking site, as shown in the lower part of Scheme I. Now the transfer may involve less efficient paths, or a longer donor–acceptor distance, or both.

Scheme I

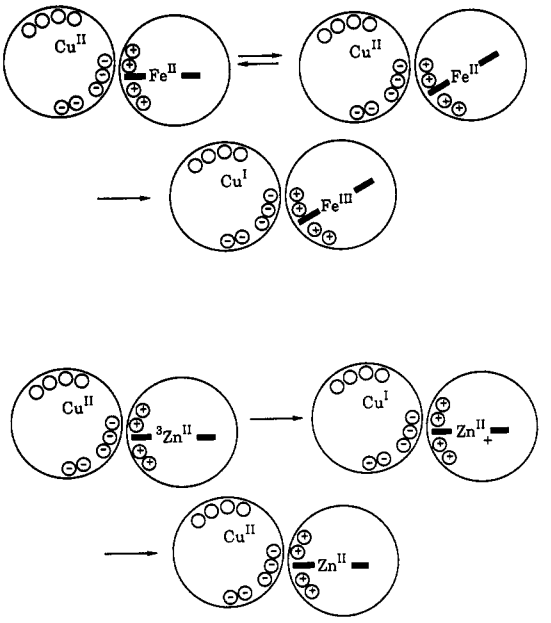


This conclusion concerning the bimolecular reactions between the protein molecules (eqs 1, 3, and 5) is supported by our previous findings on the corresponding unimolecular reactions within diprotein complexes (eqs 2, 4, and 6, respectively). Protein–protein orientation in a bimolecular reaction can be deduced from the analysis of dipolar orientations, as in this study; the orientation in a unimolecular reaction can be deduced from the comparisons of isostructural electrostatic and covalent complexes, as in our previous studies. In the presence of a carbodiimide, direct amide bonds are formed between amino groups (lysine residues) near the exposed heme edge and carboxylic groups (acidic residues) in the acidic patch. This noninvasive cross-linking captures the electrostatic diprotein complex in its initial (docking) orientation (Zhou et al., 1992). The intracomplex reaction in eq 2 in the electrostatic complex is abolished upon cross-linking (Peerey & Kostić, 1989; Peerey et al., 1991), while the intracomplex reactions in eqs 4 and 6 which are not abolished occur in both covalent and electrostatic complexes (Zhou & Kostić, 1991b, 1992a).

## CONCLUSIONS

Monopole–dipole and dipole–dipole interactions must be considered in addition to the familiar monopole–monopole interactions when the charged groups in the protein molecules are asymmetrically distributed. The improvement in the fitting

of kinetic results came from this refinement of the theoretical model, not from an increase in the number of parameters, because most of the parameters are known a priori and fixed. Analysis of electrostatic interactions over a wide range of ionic strengths can reveal the overall protein–protein orientation for the reaction. In electron-transfer reactions this orientation may depend not only on the electrostatic, hydrophobic, and other interactions between the protein molecules but also on the thermodynamic driving force or the electronic structure of the redox-active metal sites.

## ACKNOWLEDGMENT

We thank Professor Scott H. Northrup for his program for computation of dipole moments and Dr. Victoria A. Roberts for calculation of the radius of the cyt/pc complex.

## SUPPLEMENTARY MATERIAL AVAILABLE

One figure, showing second-order kinetic plots for the forward reaction in eq 3 (1 page). Ordering information is given on any current masthead page.

## REFERENCES

Anderson, G. P., Sanderson, D. G., Lee, C. H., Durell, S., Anderson, L. B., & Gross, E. L. (1987) *Biochim. Biophys. Acta 894*, 386.

Armstrong, G. D., Chapman, S. K., Sisley, M. J., Sykes, A. G., Aiken, A., Osheroff, N., & Margoliash, E. (1986) *Biochemistry 25*, 6947.

Augustin, M. A., Chapman, S. K., Daview, D. M., Sykes, A. G., Speck, S. H., & Margoliash, E. (1983) *J. Biol. Chem. 258*, 6405.

Bagby, S., Driscoll, P. C., Goodall, K. G., Redfield, C., & Hill, H. A. O. (1990) *Eur. J. Biochem. 188*, 413.

Beratan, D. N., Onuchic, J. M., & Gray, H. B. (1991) *Met. Ions Biol. Syst. 27*, 97.

Betts, J. N., Beratan, D. N., & Onuchic, J. N. (1992) *J. Am. Chem. Soc. 114*, 4043.

Brothers, H. M., II, Zhou, J. S., & Kostić, N. M. (1993) *J. Inorg. Organomet. Polym. 3*, 59.

Burkey, K. O., & Gross, E. L. (1981) *Biochemistry 20*, 5495.

Burkey, K. O., & Gross, E. L. (1982) *Biochemistry 21*, 5886.

Bushnell, G. W., Louie, G. V., & Brayer, G. D. (1990) *J. Mol. Biol. 214*, 585.

Chapman, S. L., Knox, C. V., & Sykes, A. G. (1984) *J. Chem. Soc., Dalton Trans.*, 2775.

Christensen, H. E. M., Conrad, L. S., Mikkelsen, K. V., Nielsen, M. K., & Ulstrup, J. (1990) *Inorg. Chem. 29*, 2808.

Dixit, S. N., Waring, A. J., & Vanderkooi, J. M. (1981) *FEBS Lett. 125*, 86.

Dixit, B. P. S. N., Moy, V. T., & Vanderkooi, J. M. (1984) *Biochemistry 23*, 2103.

Dixon, D. W., & Hong, X. (1990) *Adv. Chem. Ser. 226*, 162.

Dixon, D. W., Hong, X., & Woehler, S. E. (1989) *Biophys. J. 56*, 339.

Dixon, D. W., Hong, X., Woehler, S. E., Mauk, A. G., & Sishta, B. P. (1990) *J. Am. Chem. Soc. 112*, 1082.

Eigen, M., & Hammes, G. G. (1963) *Adv. Enzymol. 25*, 1.

Elias, H., Chou, M. H., & Winkler, J. R. (1988) *J. Am. Chem. Soc. 110*, 429.

Eltis, L. D., Herbert, R. G., Barker, P. D., Mauk, A. G., & Northrup, S. H. (1991) *Biochemistry 30*, 3663.

Geren, L. M., Stonehuerner, J., Davis, D. J., & Millett, F. (1983) *Biochim. Biophys. Acta 724*, 62.

Glasstone, S., Laidler, K. J., & Eyring, H. (1940) *Theory of Rate Processes*, McGraw Hill, New York.

Guss, J. M., & Freeman, H. C. (1983) *J. Mol. Biol. 169*, 521.

Hoffman, B. M., Natan, M. J., Nocek, J. M., & Wallin, S. A. (1991) *Struct. Bonding 75*, 86.

Horie, T., Maniara, G., & Vanderkooi, J. M. (1985) *FEBS Lett. 177*, 287.

King, G. C., Binstead, R. A., & Wright, P. E. (1985) *Biochim. Biophys. Acta 806*, 262.

Koppenol, W. H., & Margoliash, E. (1982) *J. Biol. Chem. 257*, 4426.

Koppenol, W. H., Rush, J. D., Mills, J. D., & Margoliash, E. (1991) *Mol. Biol. Evol. 8*, 545.

Kostić, N. M. (1991) *Met. Ions Biol. Syst. 27*, 129.

Magner, E., & McLendon, G. (1989) *J. Phys. Chem. 93*, 7130.

Marcus, R. A., & Sutin, N. (1985) *Biochim. Biophys. Acta 811*, 265.

Mauk, A. G. (1991) *Struct. Bonding 75*, 131.

McCammon, J. A., Wolynes, P. G., & Karplus, M. (1979) *Biochemistry 18*, 927.

McLendon, G. (1991a) *Struct. Bonding 75*, 160.

McLendon, G. (1991b) *Met. Ions Biol. Syst. 27*, 183.

McLendon, G., & Hake, R. (1992) *Chem. Rev. 92*, 481.

Milne, P. R., & Wells, J. R. E. (1970) *J. Biol. Chem. 245*, 1566.

Modi, S., He, S., Gray, J. C., & Bendall, D. S. (1992a) *Biochim. Biophys. Acta 1101*, 64.

Modi, S., Nordling, M., Lundberg, L. G., Hansson, Ö., & Bendall, D. S. (1992b) *Biochim. Biophys. Acta 1102*, 85.

Moore, G. R., & Pettigrew, G. W. (1990) *Cytochromes c: Evolutionary, Structural and Physicochemical Aspects*, Springer-Verlag, Berlin.

Moore, G., Williams, R. J. P., Chien, J. C. W., & Dickinson, L. C. (1980) *J. Inorg. Biochem. 12*, 1.

Moser, C. C., Keske, J. M., Warncke, K., Farid, R. S., & Dutton, P. L. (1992) *Nature 355*, 796.

Northrup, S. H., Pear, M. R., Morgan, J. D., McCammon, J. A., & Karplus, M. (1981) *J. Mol. Biol. 153*, 1087.

Northrup, S. H., Reynolds, J. C. L., Miller, C. M., Forrest, K. J., & Boles, J. O. (1986) *J. Am. Chem. Soc. 108*, 8162.

Peerey, L. M., & Kostić, N. M. (1989) *Biochemistry 28*, 1861.

Peerey, L. M., Brothers, H. M., II, Hazzard, J. T., Tollin, G., & Kostić, N. M. (1991) *Biochemistry 30*, 9297.

Pettigrew, G. W., & Moore, G. R. (1987) *Cytochromes c: Biological Aspects*, Springer-Verlag, Berlin.

Qin, L., & Kostić, N. M. (1992) *Biochemistry 31*, 5145.

Qin, L., & Kostić, N. M. (1993) *Biochemistry* (in press).

Roberts, V. A., Freeman, H. C., Getzoff, E. D., Olson, A. J., & Tainer, J. A. (1991) *J. Biol. Chem. 266*, 13431.

Rush, J. D., Lan, J., & Koppenol, W. H. (1987) *J. Am. Chem. Soc. 109*, 2679.

Rush, J. D., Levine, F., & Koppenol, W. H. (1988) *Biochemistry 27*, 5876.

Sykes, A. G. (1991a) *Adv. Inorg. Chem. 36*, 377.

Sykes, A. G. (1991b) *Struct. Bonding 75*, 177.

Therien, M. J., Chang, J., Raphael, A. L., Bowler, B. E., & Gray, H. B. (1991) *Struct. Bonding 75*, 110.

van Leeuwen, J. W. (1983) *Biochim. Biophys. Acta 743*, 408.

van Leeuwen, J. W., Mofers, F. J. M., & Veerman, E. C. I. (1981) *Biochim. Biophys. Acta 635*, 434.

Vanderkooi, J. M., & Erecinska, M. (1975) *Eur. J. Biochem. 60*, 199.

Vanderkooi, J. M., Adar, F., & Erecinska, M. (1976) *Eur. J. Biochem. 64*, 381.

Vos, K., Lavalette, D., & Visser, A. J. W. G. (1987) *Eur. J. Biochem. 169*, 269.

Wherland, S., & Gray, H. B. (1977) in *Biological Aspects of Inorganic Chemistry* (Dolphin, D., Ed.) p 289, Wiley, New York.

Winkler, J. R., & Gray, H. B. (1992) *Chem. Rev. 92*, 369.

Wuttke, D. W., Bjerrum, M. J., Winkler, J. R., & Gray, H. B. (1992) *Science 256*, 1007.

Zhou, J. S., & Kostić, N. M. (1991a) *J. Am. Chem. Soc. 113*, 6067.

Zhou, J. S., & Kostić, N. M. (1991b) *J. Am. Chem. Soc. 113*, 7040.

Zhou, J. S., & Kostić, N. M. (1992a) *J. Am. Chem. Soc. 114*, 3562.

Zhou, J. S., & Kostić, N. M. (1992b) *Biochemistry 31*, 7543.

Zhou, J. S., Brothers, H. M., II, Neddersen, J. P., Cotton, T. M., Peerey, L. M., & Kostić, N. M. (1992) *Bioconjugate Chem. 3*, 382.